JOURNAL OF Materials CHEMISTRY

Structural and electrochemical characteristics of nano-structured $Li_{0.53}Na_{0.03}MnO_2$ manganese oxide prepared by the sol–gel method

S. H. Park,[a] Y.-K. Sun,*[a]† C. S. Yoon,[b] C.-K. Kim[b] and J. Prakash[c]

[a]*Department of Chemical Engineering, Hanyang University, Seoul 133-791, Korea*
[b]*Division of Materials Science and Engineering, Hanyang University, Seoul 133-791, Korea*
[c]*Department of Chemical and Environmental Engineering, Illinois Institute of Technology, Chicago, IL 60616, USA*

Received 16th April 2002, Accepted 27th August 2002
First published as an Advance Article on the web 18th September 2002

$Li_{0.53}Na_{0.03}MnO_2$ compound was prepared by ion exchange from $Na_{0.7}MnO_2$ which was synthesized by the sol–gel method using glycolic acid as a chelating agent. Powder X-ray diffraction and transmission electron microscopy (TEM) confirmed the structure of the as-prepared material resembled that of spinel with a high degree of disorder in the (111) planes. The material delivered a discharge capacity of 200 mA h g^{-1} after 50 cycles and showed excellent cyclability without undergoing the typical capacity fading exhibited by normal spinel material. It is speculated that the stacking disorder and small particle size of the prepared $Li_{0.53}Na_{0.03}MnO_2$ powder have contributed to prevent the symmetry-breaking transformation which is believed to be responsible for capacity fading.

1. Introduction

Lithium containing transition metal oxides $LiMO_2$ (M = Co, Ni, Mn) and the spinel $LiMn_2O_4$ have been extensively studied as a cathode material for commercial lithium secondary batteries. The manganese-based oxides are promising candidates for the cathode because of their low cost, abundance and nontoxicity.[1,2] However, a wide use of the cubic spinel material has been limited due to the capacity fading observed during the extended lithium intercalation–de-intercalation cycling. In the charge and discharge processes, lithium ions are reversibly inserted into and extracted out of the $Li_xMn_2O_4$ spinel phase in two composition ranges, $0 \leqslant x \leqslant 1$ and $1 \leqslant x \leqslant 2$ which produce two voltage plateaux at 4 V and 3 V.[3,4] The spinel $LiMn_2O_4$ typically exhibit considerable capacity fading when cycled in both the 3 V and 4 V region. It has been proposed that the reasons for the capacity fading are oxidation of the organic electrolyte, structural degradation resulting from dissolution of MnO, and severe crystallographic Jahn–Teller dissolution due to high-spin Mn^{3+} ions.[5–7]

Recently, layered $LiMnO_2$ has been intensively investigated as a new layered cathode material since it has a high theoretical discharge capacity (285 mA h g^{-1}). To harness such a large theoretical discharge capacity for the $LiMnO_2$, many research groups have attempted to prepare monoclinic $LiMnO_2$ (m-$LiMnO_2$) with O3 (α-$NaFeO_2$) structure and orthorhombic $LiMnO_2$ (o-$LiMnO_2$). However, both the m- and o-$LiMnO_2$ transform into a stable spinel phase through minor cationic rearrangements that occur during the first removal and subsequent cycling of Li, leading to degradation of the electrode performance. In order to stabilize the layer structure, many research groups have studied Mn-substituted $Li_xM_yMn_{1-y}O_2$ (M = Al, Cr, Co, Ni, Li, Ti, Mg).[8–13]

Recently, an ion-exchange method has been applied to the preparation of layered lithium manganese oxide. Parant *et al.*[13] suggested a phase diagram for Na_xMnO_2 and showed that sodium manganese oxides are stable in many different structures. According to Delmas *et al.*, three different types of layered A_xMnO_y bronzes exist, distinguished by the stacking of the oxygen; (i) ABCABC, O3 type, (ii) ABBA, P2 type, and (iii) ABBCCA, P3 type. The structures are designated by a letter which refers to the oxygen environment of the alkali ion (octahedral: O, prismatic: P) followed by a number indicating the number of MO_2 sheets within the unit cell.[14,15] Paulsen *et al.*[12] reported that the high temperature O2-type $Li_{\frac{2}{3}}[Ni_{\frac{1}{3}}Mn_{\frac{2}{3}}]O_2$ was prepared by ion exchange from P2-type $Na_{\frac{2}{3}}[Ni_{\frac{1}{3}}Mn_{\frac{2}{3}}]O_2$. The O2-type structure showed a large capacity over 180 mA h g^{-1} and good capacity retention. Quine *et al.*[16] also reported that O3-type $Li_xMn_{0.95}Ni_{0.05}O_2$ prepared by ion exchange from $Na_xMn_{0.95}Ni_{0.05}O_2$ had a reversible capacity of 200 mA h g^{-1}, although the material slowly transformed to a spinel-like structure.

In this work, a sol–gel method was employed to prepare $Na_{0.7}MnO_2$ powders using glycolic acid as a chelating agent at a low calcination temperature to produce a Li-intercalated layered structure. In the process, we have discovered a pseudo-spinel structure with a high defect density whose final formula is $Li_{0.53}Na_{0.03}MnO_2$. The material unlike previously reported results showed excellent capacity retention. The electrochemical properties of the new material are presented together with detailed transmission electron microscopy work that show structural evolution during the synthesis and cycling process.

2. Experimental

$Na_{0.7}MnO_2$ powders were synthesized using a sol–gel method with glycolic acid as the chelating agent. $Na(CH_3COO)\cdot 3H_2O$ and $Mn(CH_3COO)_2\cdot 4H_2O$ (cationic ratios of Na : Mn = 0.7 : 1.0) were dissolved in distilled water, and added dropwise to a continuously stirred aqueous solution of glycolic acid. The molar ratio of glycolic acid to total metal ions was unity. The solution pH was adjusted to 7–8 using ammonium hydroxide. The resulting solution was evaporated at 70–80 °C until a transparent sol appeared. As the water evaporated further, the sol turned into a viscous transparent gel. The resulting gel precursors were decomposed at 400 °C for 5 h in air to eliminate the organic moiety and calcined at 600 °C for 12 h in air.

The prepared precursor, $Na_{0.7}MnO_2$ powders, was introduced into a mixed solution of ethanol and lithium bromide.

†Present adress: Department of Chemical and Environmental Engineering, Illinois Institute of Technology, Chicago, IL 60616, USA.

The ion exchange of Na in $Na_{0.7}MnO_2$ with Li was carried out at 80 °C for 5 h in the solution. After the reaction, the solution was filtered using vacuum suction filtering equipment and the remaining powder was washed with ethanol. The washed powder was dried at 180 °C for one day in a vacuum oven.

The concentration of lithium, sodium, and manganese was measured using the inductively coupled plasma (ICP) method by dissolving the powder in dilute nitric acid. Powder X-ray diffraction (XRD, Rigaku, Rint-2000) using Cu-Kα radiation was employed to characterize the structural properties of the powders before and after the electrochemical tests. The microstructures of the individual oxide particles were also investigated by transmission electron microscopy (TEM, JEOL 2010).

The electrochemical properties of the synthesized powders were performed in CR2030 button type cells. For the fabrication of the electrodes, the synthesized powder (20 mg) was added to a mixture of carbon black and poly(tetrafluoroethylene) (12 mg); the mixture was then pressed onto stainless Ex-met. An excess amount of lithium foil was used as the anode. The electrolyte was a 1 : 2 (v/v) mixture of ethylene carbonate (EC) and dimethyl carbonate (DMC) containing 1 M $LiPF_6$. The charge–discharge test was performed galvanostatically at a current density of 0.4 mA cm^{-2} (C/5 rate) with cutoff potentials of 2.4 to 4.5 V (*vs.* Li/Li^+).

Results and discussion

Shown in Fig. 1(a) is the XRD pattern of $Na_{0.7}MnO_2$ calcined at 600 °C 1h before ion exchange. In Fig. 1(b) is the XRD pattern of the powder obtained after ion-exchanging $Na_{0.7}MnO_2$ with LiBr in ethanol. Its chemical formula was determined through ICP analysis to be $Li_{0.53}Na_{0.03}MnO_2$. Comparing the XRD data in Fig. 1(a) and (b), the peak at 16° in the initial sodium manganese oxide has disappeared after the ion-exchange, indicating that Li-intercalation was nearly complete. The XRD pattern of the electrode after 50 cycles in Fig. 1(c) does not show much structural change after cycling. In order to demonstrate the difficulty in determining the structure of the ion-exchanged compound, also presented in Fig. 1 are the XRD patterns for the $LiNiO_2$ and $LiMn_2O_4$ powders prepared at 750 °C in an O_2 atmosphere by the sol–gel route. We have already reported their electrochemical and structural properties.[17,18] As can be seen, the $R\bar{3}m$ layered structure of $LiNiO_2$ and the spinel $LiMn_2O_4$ have nearly identical XRD patterns due to similar local atomic arrangement in both structures. Ohzuku *et al.* have shown that a simple cubic lattice can also generate a similar XRD pattern.[19] The distinguishing feature of the layered structure is the splitting of two 108 and 110 peaks at 64.2° and 64.7° (Cu-Kα) in $LiNiO_2$, which coincides with the 440 peak of the cubic spinel structure of $LiMn_2O_4$. It is, however, difficult to differentiate the two structures if the lattice is disordered such that the fine details such as splitting of the high order peaks at 64° are blurred due to line broadening. The XRD pattern of the as-prepared $Li_{0.53}Na_{0.03}MnO_2$ appears to be highly disordered judging from the broadened peaks, showing a high density of stacking disorder. We were unable to clearly distinguish the layered structure obtained by ion-exchange from the spinel phase based on the X-ray diffraction patterns alone. It is difficult to obtain a clean diffraction pattern of the ion-exchanged samples due to the high degree of structural disorder induced by the chemical exchange process and the small particle size resulting from the sol–gel process.[20,21] In addition, because of the relatively low calcination temperature, the crystallinity of the $Na_{0.7}MnO_2$ is rather poor as evidenced by the electron diffraction patterns shown in Fig. 2(b) and (c).

In order to clarify the structure of the as-prepared $Li_{0.53}Na_{0.03}MnO_2$ powder, we have utilized TEM. Since it is not possible to synthesize the spinel structure from P2 $Na_{0.7}MnO_2$ by ion exchange alone, the microstructure of the $Na_{0.7}MnO_2$ powder prior to the ion exchange was first examined. Indexing of the ring pattern of the particle cluster shown in Fig. 2(a) indicates the prepared $Na_{0.7}MnO_2$ has a spinel structure (*Fd*3*m*) with a lattice parameter of ~10.0 Å. Although the spinel structure has many overlapping diffraction peaks with the alternative structural model of P2 ($P6_3/mmc$),

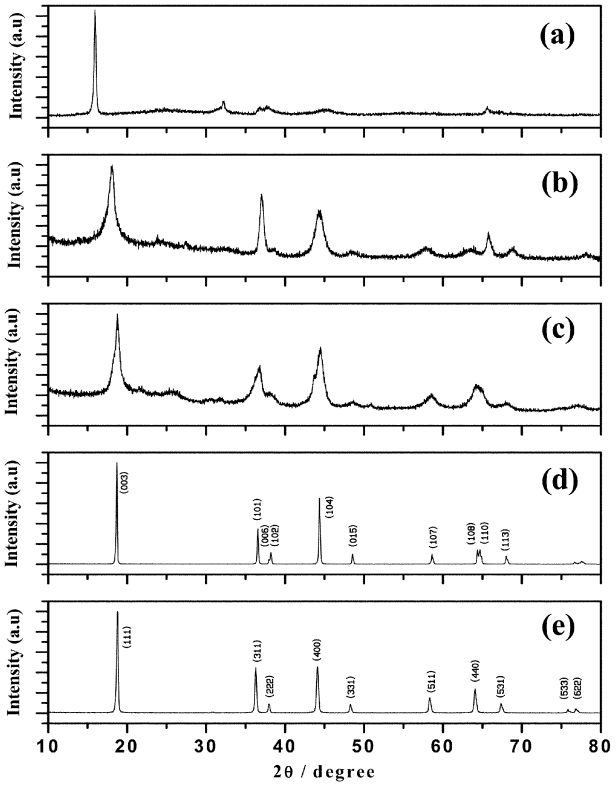

Fig. 1 X-Ray diffraction patterns for (a) $Na_{0.7}MnO_2$, (b) $Li_{0.53}Na_{0.03}MnO_2$, (c) the $Li_{0.53}Na_{0.03}MnO_2$ electrode after 50 cycles, (d) $LiNiO_2$, and (e) $LiMn_2O_4$ compounds prepared using the sol–gel method.

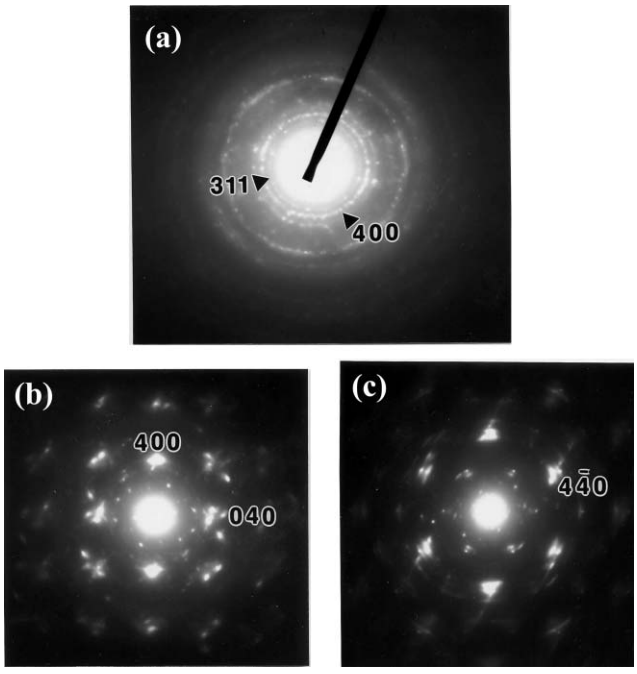

Fig. 2 Electron diffraction patterns for $Na_{0.7}MnO_2$: (a) polycrystalline ring patterns, (b) [001] zone, (c) [111] zone.

close analysis of the pattern showed that the diffraction pattern better matched that of the spinel structure. Single crystal diffraction patterns are also obtained from individual particles and shown in Fig. 2(b) and (c). The diffraction pattern in Fig. 2(b) is the spinel structure in the [001] zone with split diffraction spots, which suggests that the spinel structure of the particle is highly distorted with sub-particle domains.[22] Shown in Fig. 2(c) is the pattern of a different $Na_{0.7}MnO_2$ particle along the [111] zone. Similar to the pattern in Fig. 2(b), the diffraction peaks are split and streaked indicating disorder in both the stacking sequence and spacing. The diffraction pattern in Fig 2(b) is of a typical high-symmetry zone of cubic structure, which does not exist in P2 $Na_{0.7}MnO_2$. Although the six-fold symmetry can be seen in the [001] zone of the P2 structure, $Na_{0.7}MnO_2$ (a = 2.867 Å, c = 11.154 Å[12]) has a lattice spacing of 2.48 Å for the 001 planes which is too large to match the pattern in Fig. 2(c). The single crystal electron diffraction of particles showed that the $Na_{0.7}MnO_2$ powder prepared at a low temperature closely resembled the spinel structure with a high degree of structural defects.

Since the initial $Na_{0.7}MnO_2$ powder is spinel-like, it is likely that the ion exchanged $Li_{0.53}Na_{0.03}MnO_2$ powder will also assume the spinel structure. Shown in Fig. 3(a) is the ring pattern obtained from the $Li_{0.53}Na_{0.03}MnO_2$ powder. The pattern was indexed as belonging to the spinel structure. Again, the spinel structure is very difficult to distinguish from the O3 type $Na_{0.7}MnO_2$ with $R\bar{3}m$ symmetry using the polycrystalline ring pattern alone. The single crystal pattern of the as-prepared $Li_{0.53}Na_{0.03}MnO_2$ particle in Fig. 3(b) clearly shows the 4-fold symmetry unique to the cubic (or tetragonal) structure. To further prove that the pattern in Fig. 3(b) was generated from the spinel structure, the calculated diffraction patterns for the spinel [001] and the O3 [441] zones are shown in Fig. 3(c). The 400 peak of the spinel nearly coincides with 014 peak of the O3 structure both in intensity and position of the peak. The 104 peak is 89.2° away from the $10\bar{4}$ peak, which would have produced the [$44\bar{1}$] zone diffraction pattern resembling the experimental pattern of Fig. 3(b). However, both 014 and $10\bar{4}$ spots should be absent from the pattern due to the $-h + k + l = 3n$ reflection condition of the $R\bar{3}m$ symmetry, thus generating the pattern shown in Fig. 3(c). We have surveyed a number of

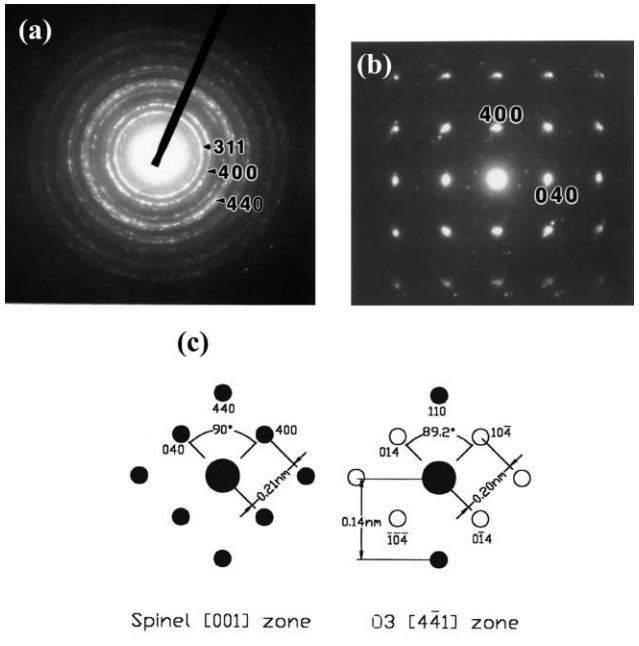

Fig. 3 Electron diffraction patterns of as-prepared $Li_{0.53}Na_{0.03}MnO_2$: (a) polycrystalline ring patterns, (b) diffraction patterns of the [001] zone, (c) calculated diffraction patterns of spinel [001] and O3 [441] zones.

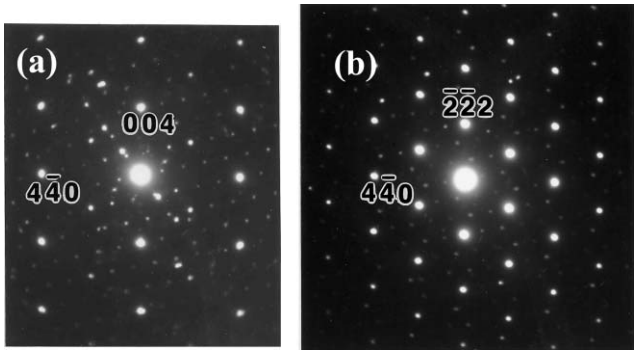

Fig. 4 Electron diffraction patterns for the as-prepared $Li_{0.53}Na_{0.03}MnO_2$ powder: (a) [110] zone, (b) [112] zone.

particles and all of the surveyed particles conformed to the spinel symmetry.

Although the as-prepared powder possesses the cubic symmetry, the structure is heavily faulted with stacking faults in the [111] direction. The diffraction patterns of the $Li_{0.53}Na_{0.03}MnO_2$ in Fig. 4(a) and (b) are taken along the [110] and [112] directions, respectively. Only 400 and 440 spots are seen in the [110] zone pattern whereas the normal spinel has an array of 200, 220, and 111 peaks. Although the 200 peak is crystallographically forbidden and the intensity of the 220 peak is supposed to be low for the spinel, the electron diffraction pattern along [110] direction typically contains those peaks arising from the double diffraction of the 111 peak.[23] Fig. 4(b) also confirms the missing 111 and 220 spots which normally appear in the [112] zone pattern. The absence of the 111 peaks and the corresponding double diffraction spots suggest that the structure is highly disordered in the (111) planes. It appears that the disorder in the stacking sequence was retained from the original $Na_{0.7}MnO_2$ structure, which had a high density of stacking faults.

Fig. 5(a) shows the discharge capacities for the $Li_{0.53}Na_{0.03}MnO_2$ electrode as a function of the number of cycles with the corresponding charge–discharge curves in Fig. 5(b). The initial discharge curves exhibited a plateau in the 3 V region. The plateau at 3 V is typical of the spinel structure and can also be observed during the first few cycles of Li_xMnO_2 (O3 type layered) or orthorhombic $LiMnO_2$ cathodes.[10,16] With further cycling, the voltage profiles started to develop another plateau at 4 V. The 4 V plateau is characteristic of the spinel phase, $LiMn_2O_4$, in which lithium ions are intercalated into tetrahedral sites over the 4 V plateau. Notice that the 4 V plateau becomes increasingly flatter after 20 cycles, which suggests that the cathode has slowly transformed into a defect-free spinel structure. This observation is in agreement with previous reports that layered Li_xMnO_2 was transformed to the spinel phase during lithium ion de-intercalation.[24,25] Recently, Quine *et al.* also reported that layered $Li_xMn_{1-y}Ni_yO_2$ with the O3 (α-$NaFeO_2$) structure delivers a high capacity of 220 mA h g^{-1} at a voltage of 2.4–4.8 V but the cycled electrode transformed to a spinel-like structure after scores of cycling.[16] Although the $Li_{0.53}Na_{0.03}MnO_2$ electrode was transformed to the spinel structure during cycling, the material showed excellent cycling performance. The electrode initially delivered a discharge capacity of 180 mA h g^{-1} which gradually increases with cycling to reach 200 mA h g^{-1} after 50 cycles (Fig. 5(a)). It is speculated that the excellent cycling behavior of the $Li_{0.53}Na_{0.03}MnO_2$ electrode can partly be attributed to the remaining small sodium content. It is highly possible that the sodium content provides a pillaring effect. Sharma *et al.* reported that the M_xMnO_2 phase is stabilized by incorporating pillar cations such as alkali metal ions.[25]

In order to verify whether or not the electrochemical properties of $Li_{0.53}Na_{0.03}MnO_2$ are the same as those of

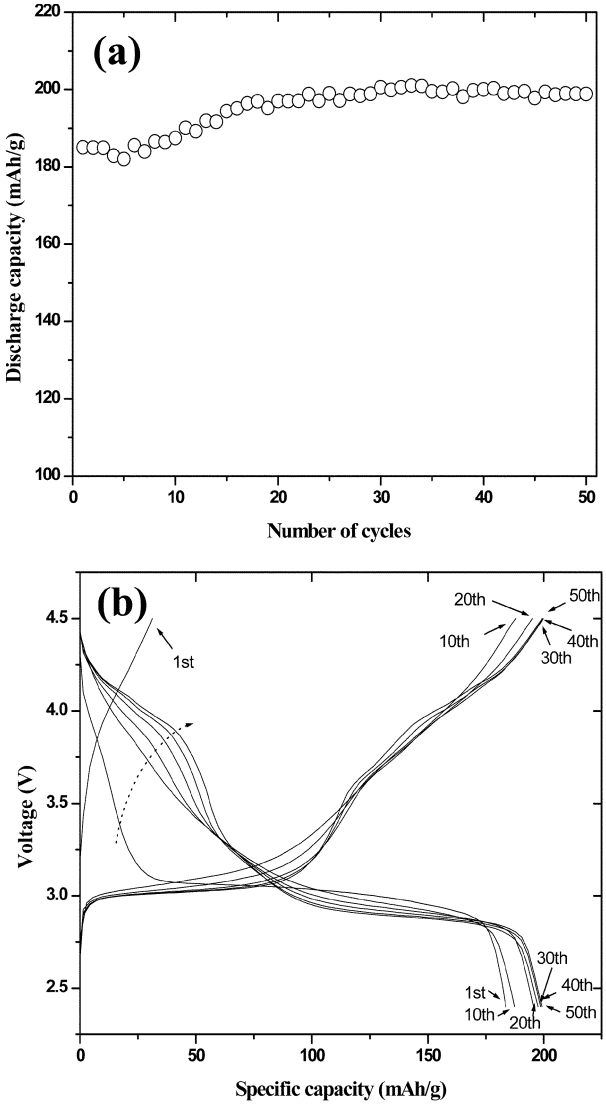

Fig. 5 (a) Charge–discharge curves at room temperature (25 °C), (b) discharge capacity of $Li_{0.53}Na_{0.03}MnO_2$ powder. Rate = 0.2 C.

normal cubic spinel, $LiMn_2O_4$, dQ/dE measurements of the samples were carried out and are shown in Fig. 6. Normal spinel $LiMn_2O_4$ has two clear redox couples at 3.95 V and 4.1 V.[19] Our $Li_{0.53}Na_{0.03}MnO_2$ material, however, has only one redox peak in the voltage range as can be seen from Fig. 6. The

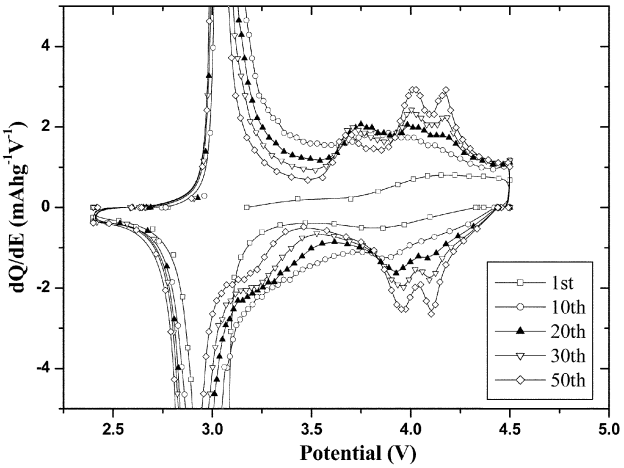

Fig. 6 Differential capacity *vs.* voltage for the $Li_{0.53}Na_{0.03}MnO_2$ cell.

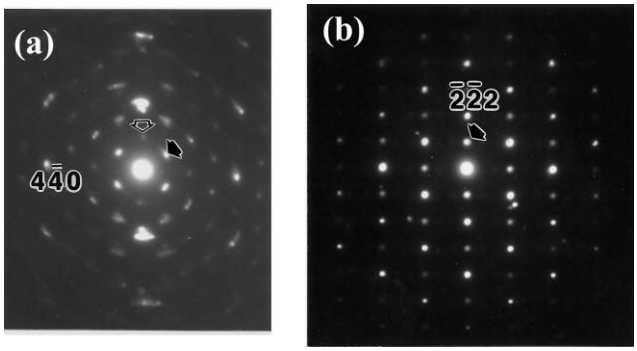

Fig. 7 Electron diffraction patterns for the $Li_{0.53}Na_{0.03}MnO_2$ electrode after 50 cycles (a) [110] zone, (b) [112] zone.

single redox peak gradually divides into two redox peaks after the 20th cycling. The result is indicative of the fact that the defects in the initial $Li_{0.53}Na_{0.03}MnO_2$ powder has been annihilated during the electrochemical cycling and the structure of the cathode has become closer to a perfect spinel structure.

Shown in Fig. 7(a) and (b) are the electron diffraction patterns of the $Li_{0.53}Na_{0.03}MnO_2$ powder after 50 electrochemical cycles taken along the [110] and [112] directions. Unlike the patterns in Fig. 4(a) and (b), the diffraction patterns now contain the 111 and 220 spots as indicated in the diffraction pattern. The patterns in Fig. 7 nearly match those of a perfect spinel structure. From the electron diffraction analysis, in agreement with the dQ/dE measurements, it can be concluded that the electrochemical cycling has removed the structural disorder in the (111) planes that is induced in the ion-exchange process.

It is not clear why the $Li_{0.53}Na_{0.03}MnO_2$ powder does not suffer from the capacity fading normally related to Jahn–Teller distortion even though the powder has been shown to possess spinel symmetry. It can be speculated that the highly disordered nature in the as-prepared material presents different local atomic arrangements, thus preventing the symmetry-breaking transformation. The excellent capacity retention can also be attributed to the small particle size as the average particle size of the as-prepared powder ranges from 50 to 200 nm. It has been experimentally considered that the nano-sized particles tend to improve the electrochemical chemical properties. Croguennec *et al.* have reported that the small grain sized compounds showed better cycling performance than powders with larger particle size.[26,27] Kang *et al.* also reported no significant capacity fading in the 3 V region for the nanocrystalline spinel $LiMn_2O_4$ obtained by ball milling.[28]

Conclusion

The electrochemical study of $Li_{0.53}Na_{0.03}MnO_2$ phase prepared by the sol–gel method showed that the material has a large discharge capacity of up to 200 mA h g^{-1} and exhibits an excellent cyclability. After 20 cycles, the powder behaves very much like the $Li_{1+x}Mn_2O_4$ cubic spinel; however, the excellent cycling behavior of the $Li_{0.53}Na_{0.03}MnO_2$ is in contrast to the previously reported cycling characteristics of the spinel phase. The cationic disorder due to the large density of stacking faults could induce stabilization of the spinel within the potential range of 2.4–4.5 V. The small particle size of the as-prepared powder also appears to contribute to the excellent capacity retention as previously reported by other researchers.

Acknowledgements

This work was supported in part by the Ministry of Information & Communication of Korea ("Support Project of

University Information Technology Research Center" supervised by KIPA).

References

1 F. Capitaine, P. Gravereau and C. Delmas, *Solid State Ionics*, 1996, **89**, 197.
2 A. R. Armstrong and P. G. Bruce, *Nature*, 1996, **381**, 499.
3 T. Ohzuku, M. Kitagawa and T. Hirai, *J. Electrochem. Soc.*, 1990, **137**, 769.
4 M. M. Thackeray, *J. Electrochem. Soc.*, 1995, **142**, 2558.
5 D. Guyomard and J. M. Tarascon, *Solid State Ionics*, 1994, **69**, 222.
6 M. M. Thackeray, *Prog. Solid State Chem.*, 1997, **25**, 1.
7 Y.-K. Sun, G.-S. Park, Y.-S. Lee, M. Yoshio and K. S. Nahm, *J. Electrochem. Soc.*, 2001, **148**, A994.
8 I. J. Davidson, R. J. McIlan, J. J. Murray and J. E. Greedan, *J. Power Sources*, 1995, **54**, 232.
9 L. Croguennec, P. Deniard and R. Brec, *J. Electrochem. Soc.*, 1997, **144**, 3323.
10 Y.-I. Jang, B. Huang, Y.-M. Chiang and D. R. Sadoway, *Electrochem. Solid-State Lett.*, 1998, **1**, 13.
11 J. M. Paulsen, R. A. Donaberger and J. R. Dahn, *Chem. Mater.*, 2000, **12**, 2257.
12 J. M. Paulsen, C. L. Thomas and J. R. Dahn, *J. Electrochem. Soc.*, 1999, **146**, 3560.
13 J. P. Parant, R. Olazcuaga, M. Devalette, C. Fouassier and P. Hagenmuller, *J. Solid Chem.*, 1971, **3**, 1.
14 C. Delmas, C. Fouassier and P. Hagenmuller, *Physica B*, 1980, **99**, 81.
15 C. Delmas, J.-J. Braconnier, A. Maazaz and P. Ilagenmuller, *Rev. Chim. Miner.*, 1982, **19**, 343.
16 T. E. Quine, M. J. Duncan, A. R. Armstrong, A. D. Robertson and P. G. Bruce, *J. Mater. Chem.*, 2000, **10**, 2838.
17 S. H. Park, K. S. Park, Y. K. Sun, K. S. Nahm, Y. S. Lee and M. Yoshio, *Electrochim. Acta*, 2001, **46**, 1215.
18 S. H. Park, K. S. Park, Y. K. Sun and K. S. Nahm, *J. Electrochem. Soc.*, 2000, **147**, 2116.
19 T. Ohzuku, S. Kitano, M. Iwanaga, H. Matsuno and A. Ueda, *J. Power Source*, 1997, **68**, 646.
20 T. Tsumura, A. Shimizu and M. Inagaki, *J. Mater. Chem.*, 1993, **3**, 995.
21 W. Liu, G. C. Farrington, F. Chaput and B. Dunn, *J. Electrochem. Soc.*, 1996, **143**, 87.
22 L. Dupont, M. Hervieu, G. Rousse, C. Masquelier, M. R. Palacin, Y. Chabre and J. M. Tarascon, *J. Solid State Chem.*, 2000, **155**, 394.
23 P. Hirsch, A. Howie, R. B. Nicholson, D. W. Pashley and M. J. Whelan, *Electron Microscopy of Thin Crystals*, Robert E. Krieger Publishing Company, Huntington, NY, 1977, p. 129.
24 G. Vitins and K. West, *J. Electrochem. Soc.*, 1997, **144**, 2587.
25 P. K. Sharma, G. J. Moore, F. Zhang, P. Zavalij and M. S. Whittingham, *Electrochem. Solid-State Lett.*, 1999, **2**, 494.
26 L. Croguennec, P. Deniard, R. Brec and A. Lecerf, *J. Mater. Chem.*, 1995, **1**, 1919.
27 L. Croguennec, P. Deniard, R. Brec, P. Biensan and M. Broussely, *Solid State Ionics*, 1996, **89**, 197.d.
28 S.-H. Kang, J. B. Goodenough and L. K. Rabenberg, *Electrochem. Solid-State Lett.*, 2001, **4**, A49.